Am J Physiol Heart Circ Physiol 295: H1198–H1205, 2008.
First published July 18, 2008; doi:10.1152/ajpheart.00510.2008.

Differences in cardiac microcirculatory wave patterns between the proximal left mainstem and proximal right coronary artery

Nearchos Hadjiloizou,[1] Justin E. Davies,[1] Iqbal S. Malik,[1] Jazmin Aguado-Sierra,[2] Keith Willson,[1] Rodney A. Foale,[1] Kim H. Parker,[1] Alun D. Hughes,[1] Darrel P. Francis,[1] and Jamil Mayet[1]

[1]*International Centre for Circulatory Health, Imperial College Healthcare National Health Service Trust, St. Mary's Hospital; and* [2]*Physiological Flow Unit, Department of Bioengineering, Imperial College, London, United Kingdom*

Submitted 14 May 2008; accepted in final form 15 July 2008

Hadjiloizou N, Davies JE, Malik IS, Aguado-Sierra J, Willson K, Foale RA, Parker KH, Hughes AD, Francis DP, Mayet J. Differences in cardiac microcirculatory wave patterns between the proximal left mainstem and proximal right coronary artery. *Am J Physiol Heart Circ Physiol* 295: H1198–H1205, 2008. First published July 18, 2008; doi:10.1152/ajpheart.00510.2008.—Despite having almost identical origins and similar perfusion pressures, the flow-velocity waveforms in the left and right coronary arteries are strikingly different. We hypothesized that pressure differences originating from the distal (microcirculatory) bed would account for the differences in the flow-velocity waveform. We used wave intensity analysis to separate and quantify proximal- and distal-originating pressures to study the differences in velocity waveforms. In 20 subjects with unobstructed coronary arteries, sensor-tipped intra-arterial wires were used to measure simultaneous pressure and Doppler velocity in the proximal left main stem (LMS) and proximal right coronary artery (RCA). Proximal- and distal-originating waves were separated using wave intensity analysis, and differences in waves were examined in relation to structural and anatomic differences between the two arteries. Diastolic flow velocity was lower in the RCA than in the LMS (35.1 ± 21.4 vs. 56.4 ± 32.5 cm/s, $P < 0.002$), and, consequently, the diastolic-to-systolic ratio of peak flow velocity in the RCA was significantly less than in the LMS (1.00 ± 0.32 vs. 1.79 ± 0.48, $P < 0.001$). This was due to a lower distal-originating suction wave (8.2 ± 6.6 × 10^3 vs. 16.0 ± 12.2 × 10^3 $W \cdot m^{-2} \cdot s^{-1}$, $P < 0.01$). The suction wave in the LMS correlated positively with left ventricular pressure ($r = 0.6$, $P < 0.01$) and in the RCA with estimated right ventricular systolic pressure ($r = 0.7$, $P = 0.05$) but not with the respective diameter in these arteries. In contrast to the LMS, where coronary flow velocity was predominantly diastolic, in the proximal RCA coronary flow velocity was similar in systole and diastole. This difference was due to a smaller distal-originating suction wave in the RCA, which can be explained by differences in elastance and pressure generated between right and left ventricles.

coronary artery hemodynamics; coronary blood flow; wave intensity analysis; coronary velocity

THE CORONARY ARTERIES have a unique flow velocity profile in that most blood flow occurs in diastole (11) rather than in systole, as in other systemic arteries (14). The contractile function of the heart enables it to pump blood to other organs of the body, but, in doing so, it paradoxically impedes its own blood supply. Previous studies have investigated the basis for the unique flow velocity profile, some by analyzing the flow-velocity profile in normal (16) or diseased left coronary arteries (15) and others by using invasive animal models (5, 24).

The right coronary artery (RCA) has a flow-velocity pattern that is less diastolic dominant than that of the left coronary arteries (7) and has different proximal and distal flow-velocity patterns (16). While a number of theories have been put forward to explain the features of the flow-velocity waveform in the left coronary arteries (4, 13, 24), the intra-coronary arterial waves (as opposed to flow waveforms) have not been compared between the right and left coronary arteries.

A wave is a transmitted disturbance and, in the context of the circulation, represents the exchange of elastic energy of the blood vessels with the kinetic energy of the blood. Propagation of waves from the left ventricle via the aorta (proximal originating) and from the intramural coronary microcirculation (distal- or microcirculatory originating) account for the flow and pressure waveforms seen in epicardial coronary arteries. While intramural vessels are surrounded by contractile muscle and are therefore subject to direct compression and decompression, epicardial coronary arteries run on the surface of the heart and are therefore not subject to direct compression or decompression from the contracting myocardium. Wave intensity analysis is a relatively new approach to interpreting coronary hemodynamics and can identify, separate, and quantify the waves associated with pressure and flow changes in the vascular tree (2, 25).

Since both the left main stem (LMS) and RCA are direct branches of the aorta and experience identical aortic pressure and waves from the left ventricle, we hypothesized that differences in compressive and decompressive forces in the right and left ventricle (8) would cause differences in the waves originating from the microcirculatory end of the arteries and explain the differences in the flow-velocity waveforms in the right and left coronary arteries, respectively.

In this study, we measured simultaneous pressure and flow-velocity waveforms throughout the cardiac cycle in the LMS and proximal RCA. We used wave intensity analysis to separate the aortic- and microcirculatory-originating components and showed that the differences in flow-velocity waveforms arise predominantly as a result of differences in the dominant microcirculatory suction (decompression) wave generated by the ventricle in early diastole. We also examined the anatomic, structural, and physiological differences between right and left coronary arteries as possible explanations of these differences.

Address for reprint requests and other correspondence: N. Hadjiloizou, International Centre for Circulatory Health, Imperial College Healthcare National Health Service Trust, St. Mary's Hospital, 59-61 N. Wharf Rd., London W2 1LA, UK (e-mail: n.hadjiloizou@imperial.ac.uk).

The costs of publication of this article were defrayed in part by the payment of page charges. The article must therefore be hereby marked "*advertisement*" in accordance with 18 U.S.C. Section 1734 solely to indicate this fact.

METHODS

Subject Population

Twenty subjects (mean age: 60 ± 12 yr, 9 men and 11 women) undergoing routine coronary angiography at Imperial College Healthcare National Health Service Trust (St. Mary's Hospital) were recruited (Table 1). Exclusion criteria included known ischemic heart disease, diabetes mellitus, renal impairment (plasma creatinine > 120 μmol/l), valvular pathology, or regional wall abnormalities on echocardiography. All patients gave written informed consent, and the protocol was approved by the local ethics committee. All authors had full access to the data and take full responsibility for its integrity.

Study Protocol

Cardiac catheterization was performed via the right femoral approach. The left coronary artery was intubated first with a left 6-Fr Judkins guiding catheter and assessed in standard angiographic projections. Subsequently, the RCA was intubated with a right 6-Fr Judkins guiding catheter and assessed in the left and right anterior oblique views. Further views in the cranial position were required to assess the distal end of the artery. Only patients found to have unobstructed coronary arteries underwent intracoronary hemodynamic measurements.

To assess the variation of the RCA distribution and myocardial territory supplied, two experienced independent observers defined dominance and the extent of its distribution and myocardial supply as previously described (20). The origin of the posterior descending artery (PDA), supplying the inferior part of the septum and left ventricular free wall, was used to describe coronary (anatomic) dominance. Right dominance was defined when the PDA originated from the RCA, left dominance was defined when the PDA originated from the left circumflex, and codominance was defined when both right and left coronary arteries supplied the PDA. Furthermore, (diastolic) flow dominance was calculated as the ratio of peak flow velocity in diastole to peak flow velocity in systole. Hemodynamic analyses were conducted by observers blinded to patient identities and the anatomic identity of the coronary artery. Additional coronary tree analysis was performed to determine the diameter, number of branches, and length of the right and left coronary arteries as previously described by Seiler et al. (21).

All patients received intravenous heparin (5,000 units) before the insertion of the intracoronary wires. No other drugs were administered during the procedure. Hemodynamic recordings of the pressure and velocity recordings were made through either a 0.014-in.-diameter WaveWire and FloWire simultaneously or a 0.014-in. ComboWire XT 0.0 (Volcano Therapeutics), which combines pressure and Doppler sensors at its tip (separated by <1 mm). Measurements were taken in the LMS and proximal RCA, and wires were manipulated to ensure that both pressure and flow signals were of high quality. When separate wires were used, care was taken to ensure that pressure and flow sensors were precisely aligned. Wire placement was performed by experienced interventional cardiologists using X-ray angiography to identity the catheter tips, and alignment of the two sensors was within 2 mm. At the typical wave speed in coronary arteries of 14 m/s, this would mean a temporal offset between the pressure and flow trace of <0.2 ms. This very small temporal displacement is much smaller than the sampling rate of 1 kHz and was not corrected for.

Table 1. *Patient demographics*

Patient Characteristics	
n	20
Age, yr	60±12
Women/men	11/9
Height, m	1.64±0.10
Weight, kg	73.9±13.0
Body mass index, kg/m^2	27.6±4.4
Total cholesterol, mmol/l	5.0±1.21
History of hypertension, *n*	10
Septal wall thickness, cm	1.16±0.26
History of smoking, *n*	10
Pharmacological therapy, *n*	
Aspirin	12
Clopidogrel	5
β-Blocker	7
Statin	10
Calcium channel blocker	3

Values are means ± SD; *n*, no. of patients.

Pressure, flow, and electrocardiograms were acquired for 60 s using a National Instruments DAQ-Card AI-16E-4 at 1 kHz using customized Labview software on a personal computer. We used an in vitro time calibration method to ensure that any time delays related to signal processing by the hardware were corrected. Data were analyzed offline using Matlab (Mathworks, Natick, MA) with custom-written software.

Pressure and flow-velocity signals were ensembled averaged over the entire 60-s recording period using the R wave of the QRS complex as the fiducial time point. Peak pressure, peak velocity, and the velocity time integral (the area under the curve) in systole and diastole were measured in the left coronary artery and RCA.

Assessment of Cavity Pressure

Since our study population consisted of patients with normal aortic valves and unobstructed coronary arteries, we used the measured systolic pressure in the coronary arteries as representative of left ventricular systolic cavity pressure. The Bernoulli equation was used to derive right ventricular systolic pressure from those with detectable tricuspid velocity on echocardiography (22).

Identifying the Origin and Nature of a Wave

Coronary arteries are unique in the circulation in that waves are generated from both their proximal and distal ends. The pumping action of the heart generates waves that are propagated from the left ventricular cavity into the aorta and, subsequently, into the coronary arteries (aortic- or proximal-originating waves). Since the coronary arteries supply cardiac muscle, waves are also generated in the contracting or relaxing myocardium and propagated from the distal end of the coronary arteries (distal- or microcirculatory-originating waves).

In wave intensity theory, a rise in pressure accompanies a compression wave, which has a "pushing" effect. A compression wave is an accelerating wave (increases velocity) if it originates from the proximal end of the coronary arteries, but it is a decelerating wave if it originates from the distal end of the coronary arteries (decreases velocity). A fall in pressure accompanies a decompression wave, which has a "suction" effect. Therefore, a decompression wave is a decelerating wave if it originates from the proximal end of the coronary arteries (decreases velocity), whereas if it originates from the distal end it is an accelerating wave (increases velocity; Table 2).

Separation of Proximal- and Distal-Originating Pressure Waves

The principle of separating the pressure waveform into its proximal-originating ($dP_{proximal}$) and distal-originating (dP_{distal}) components employs the "water hammer" equations that relate changes in pressure and velocity to derive *Eq. 1* and *2* as follows:

$$dP_{proximal} = \frac{1}{2}(dP + \rho c dU) \quad (1)$$

$$dP_{distal} = \frac{1}{2}(dP - \rho c dU) \quad (2)$$

where ρ is the density of blood (taken as 1,050 kg/m^3), c is wave speed, dP is the incremental change in coronary artery pressure, and dU is the incremental change in blood velocity.

Table 2. *Origin and nature of waves from simultaneous pressure and Doppler velocity measurements taken at the same location*

Pressure	Velocity	Wave Origin	Wave Nature
↑	↑	Proximal (aortic)	Accelerating
↑	↓	Distal (microcirculatory)	Decelerating
↓	↑	Distal (microcirculatory)	Accelerating
↓	↓	Proximal (aortic)	Decelerating

↑, Increase; ↓, decrease.

Calculation of Wave Speed in Coronary Arteries

Because the coronary arteries are too short to apply the conventional two-point measurement technique used in the aorta, we used the following single-point equation (*Eq. 3*) to calculate the local wave speed using simultaneous pressure and Doppler measurements:

$$c = \frac{1}{\rho}\sqrt{\frac{\Sigma dP^2}{\Sigma dU^2}} \qquad (3)$$

This technique has been validated in the aorta and applied in the coronary arteries by Davies et al. (3).

Deriving Proximal- and Distal-Originating Wave Intensity

The principle of wave intensity and derivation of individual waves has been extensively described elsewhere (2). In brief, by measuring the rate of change in pressure and of flow velocity simultaneously at the same point enabled us to describe the changes in flow in terms of travelling waves that originate from the proximal end ($WI_{proximal}$; *Eq. 4*) and the distal end (WI_{distal}; Eq. 5) of the artery, as follows:

$$WI_{proximal} = \frac{1}{4\rho c}\left(\frac{dP}{dt} + \rho c \frac{dU}{dt}\right)^2 \qquad (4)$$

$$WI_{distal} = -\frac{1}{4\rho c}\left(\frac{dP}{dt} - \rho c \frac{dU}{dt}\right)^2 \qquad (5)$$

The waves occurring at any given time in the cardiac cycle can therefore be identified and quantified and their contribution to the flow velocity profile determined: these waves can either increase flow velocity (accelerating waves) or decrease flow velocity (decelerating waves).

Quantification of Waves

Both the peak and cumulative (area under curve) wave intensity for each of the predominant proximal- and distal-originating waves was measured. Wave intensity is a measure of the instantaneous flux of energy density, whereas cumulative wave intensity is an index of the energy density of a wave. Both measures were adjusted for sampling rate, as proposed by Jones et al. (10).

Reproducibility

The reproducibility of hemodynamic measurements was calculated by examining separate 30-s recordings of blood pressure and velocity for each patient.

Statistical Analysis

The statistical package Statview 5.0 (SAS Institute, Cary, NC) was used for analysis. Continuous variables are reported as means ± SD. Comparisons were made using a paired two-tailed Student's *t*-test. A *P* value of ≤0.05 was taken as statistically significant.

Table 3. *Hemodynamic variables and structural characteristics of the LCA and RCA*

	LCA	RCA	*P* Value
Systolic blood pressure, mmHg	152±28	147±23	0.1
Diastolic blood pressure, mmHg	79±15	76±15	0.3
Heart rate, beats/min	69±12	70±14	0.4
Duration of diastole, ms	447±118	420±131	0.2
Diameter, mm	4.7±0.5	3.7±0.7	<0.0001
Length, cm	63.8±17.2	38.6±9.7	<0.0001
No. of branches	18.5±4.2	8.9±2.6	<0.0001
Wave speed, m/s	13.7±6.3	14.0±5.0	0.8

Values are means ± SD. LCA, left coronary artery; RCA, right coronary artery. Blood pressure, diameter, and wave speed measurements were taken at the proximal part of each artery. Lengths and numbers of branches were measured using the technique previously described by Seiler et al. (21). *P* values were calculated using a paired Student's *t*-test.

RESULTS

Hemodynamic Measurements

There were no differences in blood pressure or heart rate between RCA and left coronary artery recordings (Table 3). Diastolic velocity in the RCA was lower than in the LMS; systolic measurements did not differ (Table 4). There was marked diastolic flow dominance in the LMS (Table 4). In contrast, in the RCA, diastolic flow dominance (ratio > 1) was small or absent.

Reproducibility

The mean ± SD of the difference between the separate 30-s recordings of blood pressure was 1.6 ± 1.3 mmHg. The SD of the difference in pressure represented 1.6% of the average blood pressure in the two recordings. The mean ± SD of the difference between the separate 30-s recordings of flow velocity was 0.014 ± 0.018 m/s. The SD of the difference in flow velocity represented 5.5% of the average flow velocity in the two recordings.

Waves in Right and Left Epicardial Coronary Arteries

In the RCA, the same six waves were present as previously identified in the left coronary arteries (2) but their magnitudes differed, for some waves markedly (Fig. 1). Waves occurred in the same sequence during each of the cardiac cycles in all patients studied, but timings differed between subjects.

Table 4. *Velocity time integral and peak systolic and diastolic measurements in each of the coronary arteries*

	LMS	RCA	*P* Value
Velocity time integral, cm			
Systole	8.4±5.0	8.5±3.8	0.9
Diastole	17.1±8.0	9.9±4.8	<0.001
Dominance	2.19±0.60	1.26±0.43	<0.001
Peak velocity, cm/s			
Systole	31.9±17.9	36.4±17.0	0.2
Diastole	56.4±32.5	35.1±21.4	<0.002
Dominance	1.79±0.48	1.00±0.32	<0.001

Values are means ± SD. A comparison between measurements in the left main stem (LMS) and RCA is shown. Flow dominance was calculated as the ratio of peak diastolic to peak systolic velocity. *P* values were calculated using a paired Student's t-test.

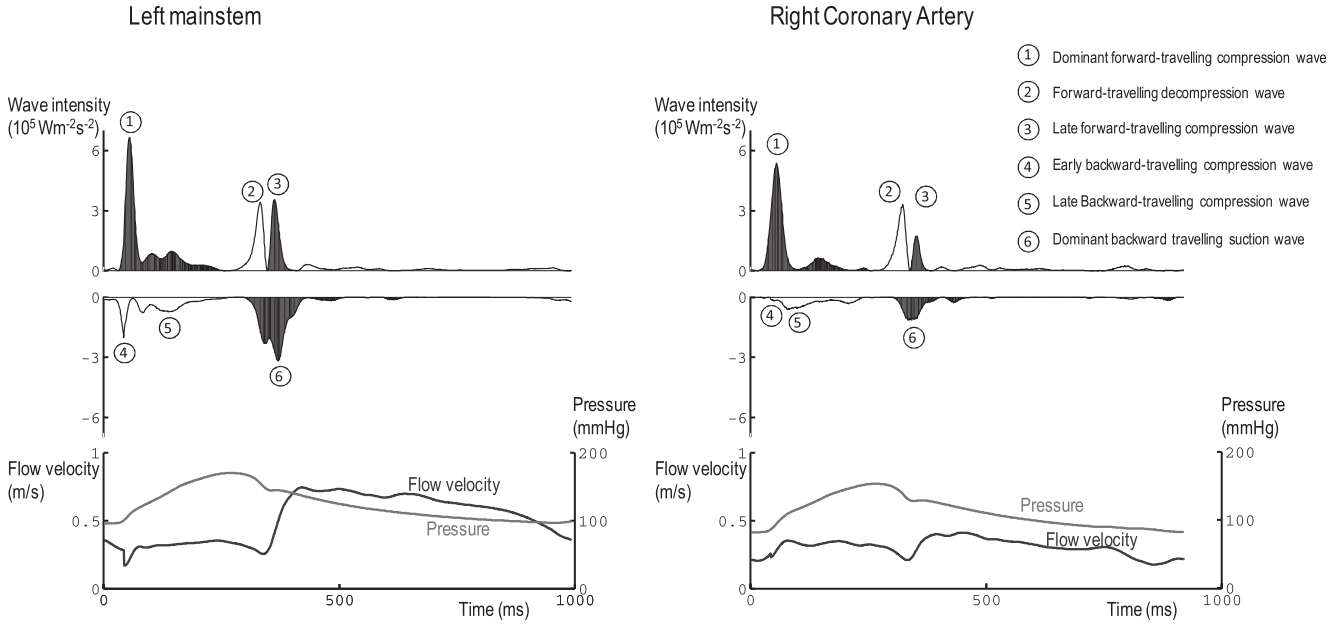

Fig. 1. Representative simultaneous pressure and flow waveforms in the left main stem and proximal right coronary artery (*bottom*) together with the respective wave intesity in each artery (*top*). Data are ensembled-averaged pressure and flow-velocity traces in 1 subject. Waves shown above the *x*-axis in the *top* originate from the aortic end; waves shown below the *x*-axis in the *top* originate from the microcirculatory end. Solid waves show accelerated flow; open waves show decelerated flow. *Waves 1–6* are described in the *inset*.

Three of these waves originated from the aortic end of the coronary artery (proximal-originating waves; Fig. 1, *waves 1–3*), and three of these waves originated from the distal end of the coronary artery (microvascular-originating waves; Fig. 1, *waves 4–6*). Proximal-originating waves are shown above the *x*-axis in Fig. 1, *top*. Distal-originating waves are shown below the *x*-axis in Fig. 1, *top*. In Fig. 1, the solid waves show accelerate velocity (acceleration waves), whereas the open waves show decelerate velocity (decelerating waves).

The first of the proximal-originating waves was the dominant forward-traveling compression wave (Fig. 1, *wave 1*); during this time, both pressure and velocity increased. The forward-traveling decompression wave is the second of the proximal-originating waves (Fig. 1, *wave 2*); during this time, both pressure and velocity decreased. At the time of the aortic notch on the pressure waveform, both pressure and velocity increased and a late forward-traveling compression wave was evident (Fig. 1, *wave 3*).

The first of the distal-originating waves was a backward-traveling compression wave. It had an early component (Fig. 1, *wave 4*) and a late component (Fig. 1, *wave 5*). During this time, pressure increased with little change in the flow velocity. The last of the distal-originating waves was the dominant backward-traveling decompression (suction) wave, which was accompanied by a decrease in pressure and an increase in velocity (Fig. 1; *wave 6*).

Comparison of Waves in Right and Left Epicardial Coronary Arteries

In the RCA, the total cumulative wave intensity arising from the microvascular end was less than the total cumulative wave intensity arising from the microvasculature in the LMS ($17.8 \pm 10.2 \times 10^{-3}$ vs. $28.4 \pm 23.1 \times 10^{-3}$ $W \cdot m^{-2} \cdot s^{-1}$, $P < 0.05$; Table 5). The largest of these distal-originating waves was the backward-traveling suction wave (occurring in diastole), and this was much smaller in the RCA than in the LMS ($8.2 \pm 6.6 \times 10^{-3}$ vs. $16.0 \pm 12.2 \times 10^{-3}$ $W \cdot m^{-2} \cdot s^{-1}$, $P < 0.01$; Table 5). During this time, diastolic velocity was less in the RCA than in the LMS (35.1 ± 21.4 vs. 56.4 ± 32.5 cm/s; Table 4). The early backward-traveling compression wave (occurring in early systole before ejection) was also smaller in the RCA than in the LMS ($0.3 \pm 0.5 \times 10^{-3}$ vs. $2.4 \pm 3.9 \times 10^{-3}$ $W \cdot m^{-2} \cdot s^{-1}$, $P < 0.04$).

The total cumulative wave intensity of the proximal-originating waves was similar between the RCA and LMS ($38.2 \pm 26.3 \times 10^{-3}$ vs. $36.4 \pm 29.0 \times 10^{-3}$ $W \cdot m^{-2} \cdot s^{-1}$, $P = 0.80$; Table 5). The largest of the proximal-originating waves was the dominant forward-traveling compression wave, and the cumulative wave intensity of this wave was not different between the RCA and LMS ($17.6 \pm 17.8 \times 10^{-3}$ vs. $12.6 \pm 9.1 \times 10^{-3}$ $W \cdot m^{-2} \cdot s^{-1}$, $P = 0.3$; Table 5). During this time, systolic velocity was not significantly different between the two arteries (36.4 ± 17.0 vs. 31.9 ± 17.9 m/s, $P = 0.2$).

What Can Account for the Differences in the Velocity Waveform in the Proximal RCA and LMS?

Structural properties. The left coronary arteries were longer and had more identifiable branches than the RCAs (Table 3). Of the 20 patients studied, 16 patients had right dominance, 3 patients had codominance, and 1 patient had left dominance. There were no differences in wave speeds between the LMS and RCA (Table 3).

The cumulative wave intensity of the backward-traveling suction wave in the RCA did not correlate with the respective vessel diameter ($r = 0.06$, $P = 0.8$), length ($r = -0.03$, $P = 0.9$), number of branches ($r = 0.12$, $P = 0.6$), or left ventricular mass ($r = -0.20$, $P = 0.4$). The cumulative wave intensity of the backward-traveling suction wave in the LMS did not

Table 5. *Wave intensity in the proximal LMS and proximal RCA*

Wave Type	Peak Wave Intensity, $\times 10^5$ W·m^{-2}·s^{-2}	Peak Wave Intensity, *P* value	Cumulative Wave Intensity, $\times 10^5$ W·m^{-2}·s^{-2}	Cumulative Wave Intensity, *P* value	Proportion of Cumulative Wave Intensity, %
Dominant forward-traveling compression wave					
LMS	5.3±2.0	0.2	12.6±9.1	0.3	26.5±7.9
RCA	7.2±7.0		17.6±17.8		36.5±14.7
Forward-traveling decompression wave					
LMS	2.8±3.3	0.6	8.1±11.5	0.7	12.9±5.4
RCA	2.5±1.9		7.5±5.7		17.8±6.9
Late forward-traveling compression wave					
LMS	1.7±1.5	0.2	3.0±2.4	0.1	6.7±4.0
RCA	1.4±1.9		2.0±2.8		3.9±2.9
Early backward-traveling compression wave					
LMS	−1.0±1.5	<0.03	−2.4±3.9	<0.04	2.7±3.0
RCA	−0.2±0.3		−0.3±0.5		0.7±0.9
Late backward-traveling compression wave					
LMS	−2.6±3.1	0.2	−14.1±20.6	0.2	20.7±4.7
RCA	−1.5±1.1		−7.6±3.9		20.1±8.2
Backward-traveling suction wave					
LMS	−4.4±3.1	<0.01	−16.0±12.2	0.01	30.8±8.0
RCA	−2.6±2.2		−8.2±6.6		20.5±8.6
Total proximal-originating cumulative wave					
LMS			36.4±29.0	0.8	56.6±6.4
RCA			38.2±26.3		66.8±6.7
Total distal-originating cumulative wave					
LMS			−28.4±23.1	<0.05	43.4±6.4
RCA			−17.8±10.2		33.2±6.7

Values are means ± SD. *P* values were calculated using a paired Student's *t*-test.

correlate with the respective vessel diameter ($r = -0.13$, $P = 0.6$). There was a weak negative correlation of the suction wave with left coronary artery length ($r = -0.47$, $P = 0.05$) and significant negative correlations with the number of branches ($r = -0.49$, $P < 0.05$) and left ventricular mass ($r = -0.52$, $P < 0.03$).

Cavity (ventricular) pressure and the backward-traveling decompression wave in diastole. The cumulative wave intensity of the backward-traveling suction wave in the LMS correlated with intra-arterial systolic pressure ($r = 0.58$, $P < 0.02$), and the cumulative wave intensity of the backward-traveling suction wave in the RCA correlated with estimated right ventricular systolic pressure ($r = 0.70$, $n = 8$, $P = 0.05$).

DISCUSSION

In this study, we confirmed that flow-velocity patterns differ between the LMS and RCA and provided a novel explanation for this difference. Using wave intensity analysis, we found that the difference in the diastolic velocity is associated with a smaller backward-traveling suction wave arising from the microvasculature in the right ventricle. Minor differences in the flow-velocity waveform in systole were associated with smaller backward-traveling compression waves particularly during isovolumic contraction, although these were of lesser importance in terms of the overall flow waveform.

Interpretation of the Origin of Waves in Right and Left Coronary Arteries

In this study, we present a new technique for the assessment of waves occurring during the cardiac cycle. To our knowledge, this is the first publication of this technique in the RCA and extends on the previous published work on the left coronary artery (2).

During ventricular contraction, a dominant forward-traveling compression wave (a forward compression wave in fluid or gas dynamics terminology; Fig. 1, *wave 1*) propagates from the aortic end as a result of left ventricular contraction and consequently rising aortic pressure. It is an accelerating wave and accounts for the increase in flow velocity in systole.

The dominant forward-traveling compression wave is preceded by a large backward-traveling compression wave originating from the microcirculatory end, which is also the result of the contracting myocardium. Since this precedes ejection, it is the result of isovolumic contraction, with the elevated cavity pressure and altered myocardial elastance causing compression of the intramyocardial vasculature and resulting in the propagation of an early backward-traveling compression wave into the epicardial arteries (Fig. 1, *wave 4*). The early backward-traveling compression wave is much larger in the left coronary arteries than in the RCA (where it is often undetectable). This is followed by another backward-traveling compression wave that is probably due to the combination of the continuation of compression of the intramyocardial vasculature and reflection of the forward-traveling wave (the late backward-traveling compression wave; Fig. 1, *wave 5*). These waves increase pressure and decelerate velocity and account for the lack of increment in flow velocity in systole.

Before closure of the aortic valve, when the rate of ventricular contraction declines, a forward-traveling decompression wave is generated by the left ventricle (Fig. 1, *wave 2*). This is followed by a late forward-traveling compression wave (Fig. 1, *wave 3*) following aortic valve closure. Both of these waves originate from the aortic end, with the former decelerating and the latter accelerating flow velocity. Both are comparatively smaller than the dominant backward-traveling suction wave (Fig. 1, *wave 6*), which occurs at the same time and originates

from the distal end of the coronary arterial tree as a result of the decompression of the intramyocardial vasculature, probably as a result of rapidly decreasing elastance and a fall in cavity pressure (28).

This large backward-traveling suction wave accounts for the early increase in flow velocity seen in diastole in the epicardial arteries. This wave was much larger in the LMS than in the RCA and accounts for the marked difference in diastolic flow (Table 4). Furthermore, the dominant forward-traveling compression wave, the largest of the proximal-originating waves, is similar between the two arteries (Table 5).

Applying Wave Intensity to Coronary Physiology

Whereas previous research, in diseased coronary arteries, has implicated both proximal and distal factors to be important in determining the flow-velocity profile in coronary arteries (9, 15, 17), our findings suggest that, in unobstructed coronary arteries, the influence on coronary flow from the distal (microcirculatory) end is predominantly responsible for the distinctive features of the flow-velocity waveform in the right and left coronary arteries (2, 24).

In all arteries, blood flows down a pressure gradient, and, in regard to mean flow, this gradient is established by the contractile action of the heart. The situation is more complex when consideration is given to the variation of flow within a cardiac cycle. Transient changes in flow, notably in the coronary arteries, can arise from pressure gradients established by events at both proximal (aortic) and distal (intramyocardial) sites.

We separated the proximal-originating (aortic) and distal-originating (microvascular) waves using wave intensity analysis. With the onset of cardiac contraction, raised chamber pressure combined with myocardial thickening compresses intramyocardial vessels and causes the distal-originating pressure to rise in early systole before the opening of the aortic valve (isovolumic ventricular contraction). This is seen as a backward-traveling compression wave that decelerates flow, particularly in the left coronary arteries (2). As cardiac contraction continues, intra-ventricular pressure rises until it exceeds pressure in the aorta. When this occurs, the aortic valve opens and ejection begins, resulting in a forward-traveling compression wave transmitted into the aorta that accelerates the forward flow of blood. At a later stage in the cardiac cycle, but before closure of the aortic valve, the rate of myocardial contraction declines and results in a forward- traveling decompression wave that slows aortic blood flow and contributes to aortic valve closure (18, 19). In itself, this wave would be anticipated to slow coronary blood flow velocity, but, at the same time, the decompression of intramyocardial vessels generates a backward-traveling decompression (suction) wave that accelerates flow and opposes the effect of the forward-traveling decompression wave. Once the aortic valve closes, the effect of the backward-traveling suction wave is unopposed and results in a marked increase in flow velocity in the left coronary artery (2). In the RCA, this suction wave is significantly smaller than in the LMS, doubtless as a consequence of lower peak cavity pressure and lesser decompression during relaxation of the myocardium. These differences in waves largely account for the different shapes of the flow-velocity waveform in these arteries.

To explore other possible determinants of the differences in diastolic velocity between the proximal RCA and LMS, we correlated the size of the suction wave with structural and anatomic differences between right and left sides. In our study, the majority of the RCAs were anatomically dominant. In view of this, the present study has limited power to address whether variations in coronary artery dominance influence the RCA waveform. However, the limited data we have do not support a major influence of anatomic dominance on the magnitude of the suction wave.

Since the wave speed in the LMA and RCA is similar, arterial wall properties are unlikely to contribute to the difference in the intramyocardial contribution. In the LMS, left ventricular mass and correlates of left ventricular mass such as coronary artery length and number of branches have a negative association with the suction wave [as previously shown (2)]. We were not able to explore possible relationships between right ventricular mass and waves in the RCA since we lacked measurements of right ventricular mass.

A plausible explanation for the difference in the contribution from the distal end (the suction wave) is that blood in the LMS and proximal RCA is subjected to active compression and decompression, which is dependent on chamber pressures and the contractile force generated by the myocardium of the respective ventricles (13, 24); in diastole, decompressive effects in the left ventricle would be expected to be larger and generate a comparatively larger suction wave. This is transmitted to the proximal LMS, whereas the lesser decompressive effects in the right ventricle would be anticipated to generate a comparatively smaller suction wave in the proximal RCA. Since the RCA does provide some blood supply to the left ventricle, this interpretation suggests that the waves seen in the proximal right and left coronary arteries better reflect the regions of the myocardium supplied by the more proximal branches. This is consistent with previous suggestions that backward propagation of waves is relatively limited (6). Overall, the findings of this study are consistent with recent models of coronary flow (13, 24) that found a key role of chamber pressures and myocardial contractility in the determination of coronary flow patterns.

Study Limitations

It is a limitation of this study that each subject had some grounds for suspicion of ischemic heart disease that merited angiography. Thus, the subjects may not be regarded as representative of healthy individuals. However, it should be stressed that all subjects had minimal symptoms, normal left ventricular function with no evidence of regional wall abnormality, and no angiographic evidence of coronary artery disease. Patients with left ventricular hypertrophy were not excluded from this study, and there is evidence that people with left ventricular hypertrophy may have coronary microvascular disease (1). Previously, we have reported that left ventricular hypertrophy is associated with a smaller distal-originating suction wave (2), and this was confirmed in the preent study. However, the inclusion of people with left ventricular hypertrophy would have tended to attenuate differences in the magnitude of the suction wave between the LMS and RCA, and we believe this limitation is unlikely to affect our conclusions.

The limitations of quantitative angiography in determining coronary lumen stenosis are well known (12). Patients underwent hemodynamic recordings only if the coronary arteries were considered to be free of disease by two operators. It is possible that subclinical atherosclerosis may have been present in some subjects. However, such subtle lesions would not be expected to affect wave propagation.

The product of changes in pressure and velocity were used to calculate wave intensity. Small variations in hemodynamics can lead to large variations in magnitude of wave energies. In our reproducibility measurements, we have shown that intrapatient variation is very small. However, the interpatient variation can often be large. We, therefore, calculated both peak and cumulative wave intensity and also represented wave intensity in terms of the percentage of the total cumulative wave intensity to facilitate interpretation of the relative contribution of each wave within each patient.

The derivation of wave speed applied the use of the single-point technique (3). The branching pattern of the coronary arteries can contribute to an overestimate of the true wave speed. To reduce this theoretical risk, we made sure that all of our recordings were taken at the proximal site of the coronary arteries, thus avoiding close proximity to branches. In our calculations, we used a single mean wave speed estimate throughout the cardiac cycle. It is likely that wave speed changes throughout the cardiac cycle, but small variations in wave speed have not been shown to change the magnitude or pattern of these waves (2). To our knowledge, the single-point technique is the only method currently available to measure wave speed in human coronary arteries.

The use of two intracoronary wires may affect blood flow and has been reported to result in an overestimation of the severity of moderate stenoses (27). However, a previous study by our group (26) suggested that the presence of a wire in normal unobstructed arteries has a relatively modest effect on blood flow, and, in any case, it is difficult to envisage how such an effect could account for differences between coronary arteries, such as those found in this study.

In our interpretation of the origin of waves in the coronary circulation, we have outlined the mechanisms most likely to generate the coronary artery wave intensity profile. While such mechanisms provide an adequate explanation, it is possible that alternative or additional interpretations may exist (23).

Conclusions

Flow-velocity waveforms differ between the LMS and proximal RCA. The lack of diastolic predominance of flow velocity in the RCA is associated with a smaller distal- originating decompression (suction) wave in early diastole. We propose that the smaller distal-originating suction wave in early diastole in the RCA compared with LMS arises from lesser decompression of the coronary microvasculature supplied by the proximal branches of these arteries during ventricular relaxation.

ACKNOWLEDGMENTS

The authors acknowledge the support of all staff at St. Mary's Hospital cardiology catheter laboratory and especially Sister Chelsea Herbert and Sister Nicky Felix.

GRANTS

The authors are grateful for support from the National Institute of Health Research Biomedical Research Centre funding scheme and the Coronary Flow Trust. N. Hadjiloizou (FS/05/34), J. E. Davies (FS/05/006), and D. P. Francis (FS/04/079) are British Heart Foundation fellows.

REFERENCES

1. **Camici PG, Crea F.** Coronary microvascular dysfunction. *N Engl J Med* 356: 830–840, 2007.
2. **Davies JE, Whinnett ZI, Francis DP, Manisty CH, guado-Sierra J, Willson K, Foale RA, Malik IS, Hughes AD, Parker KH, Mayet J.** Evidence of a dominant backward-propagating "suction" wave responsible for diastolic coronary filling in humans, attenuated in left ventricular hypertrophy. *Circulation* 113: 1768–1778, 2006.
3. **Davies JE, Whinnett ZI, Francis DP, Willson K, Foale RA, Malik IS, Hughes AD, Parker KH, Mayet J.** Use of simultaneous pressure and velocity measurements to estimate arterial wave speed at a single site in humans. *Am J Physiol Heart Circ Physiol* 290: H878–H885, 2006.
4. **Downey JM, Kirk ES.** Inhibition of coronary blood flow by a vascular waterfall mechanism. *Circ Res* 36: 753–760, 1975.
5. **Downey JM, Kirk ES.** Distribution of the coronary blood flow across the canine heart wall during systole. *Circ Res* 34: 251–257, 1974.
6. **Feng J, Long Q, Khir AW.** Wave dissipation in flexible tubes in the time domain: in vitro model of arterial waves. *J Biomech* 40: 2130–2138, 2007.
7. **Heller LI, Silver KH, Villegas BJ, Balcom SJ, Weiner BH.** Blood flow velocity in the right coronary artery: assessment before and after angioplasty. *J Am Coll Cardiol* 24: 1012–1017, 1994.
8. **Hoffman JI, Spaan JA.** Pressure-flow relations in coronary circulation. *Physiol Rev* 70: 331–390, 1990.
9. **Iwakura K, Ito H, Takiuchi S, Taniyama Y, Nakatsuchi Y, Negoro S, Higashino Y, Okamura A, Masuyama T, Hori M, Fujii K, Minamino T.** Alternation in the coronary blood flow velocity pattern in patients with no reflow and reperfused acute myocardial infarction. *Circulation* 94: 1269–1275, 1996.
10. **Jones CJ, Suguwara M, Davis RH, Kondoh Y, Uchida K, Parker KH.** *Arterial Wave Intensity: Physical Meaning and Physiological Significance*, edited by Hosoda S, Yaginuma T, Sugawara M, Taylor MG, Caro CG. Chur, Switzerland: Hanvood Academic, 1994, p. 129–148.
11. **Kajiya F, Matsuoka S, Ogasawara Y, Hiramatsu O, Kanazawa S, Wada Y, Tadaoka S, Tsujioka K, Fujiwara T, Zamir M.** Velocity profiles and phasic flow patterns in the non-stenotic human left anterior descending coronary artery during cardiac surgery. *Cardiovasc Res* 27: 845–850, 1993.
12. **Kern MJ, Dupouy P, Drury JH, Aguirre FV, Aptecar E, Bach RG, Caracciolo EA, Donohue TJ, Rande JL, Geschwind HJ, Mechem CJ, Kane G, Teiger E, Wolford TL.** Role of coronary artery lumen enlargement in improving coronary blood flow after balloon angioplasty and stenting: a combined intravascular ultrasound Doppler flow and imaging study. *J Am Coll Cardiol* 29: 1520–1527, 1997.
13. **Krams R, Sipkema P, Westerhof N.** Varying elastance concept may explain coronary systolic flow impediment. *Am J Physiol Heart Circ Physiol* 257: H1471–H1479, 1989.
14. **Nichols WW, O'Rourke MF.** McDonald's blood flow in arteries: theoretical, experimental and clinical principles. London: Hodder Arnold, 1998.
15. **Ofili EO, Kern MJ, Labovitz AJ, St Vrain JA, Segal J, Aguirre FV, Castello R.** Analysis of coronary blood flow velocity dynamics in angiographically normal and stenosed arteries before and after endolumen enlargement by angioplasty. *J Am Coll Cardiol* 21: 308–316, 1993.
16. **Ofili EO, Kern MJ, St Vrain JA, Donohue TJ, Bach R, al-Joundi B, Aguirre FV, Castello R, Labovitz AJ.** Differential characterization of blood flow, velocity, and vascular resistance between proximal and distal normal epicardial human coronary arteries: analysis by intracoronary Doppler spectral flow velocity. *Am Heart J* 130: 37–46, 1995.
17. **Okamura A, Ito H, Iwakura K, Kawano S, Inoue K, Yamamoto K, Ogihara T, Fujii K.** Usefulness of a new grading system based on coronary flow velocity pattern in predicting outcome in patients with acute myocardial infarction having percutaneous coronary intervention. *Am J Cardiol* 96: 927–932, 2005.
18. **Parker KH, Jones CJ, Dawson JR, Gibson DG.** What stops the flow of blood from the heart? *Heart Vessels* 4: 241–245, 1988.

19. **Ramsey MW, Sugawara M.** Arterial wave intensity and ventriculoarterial interaction. *Heart Vessels Suppl* 12: 128–134, 1997.
20. **Schlesinger M.** Relation of the anatomic pattern to pathologic conditions of the coronary arteries. *Arch Pathol* 30: 403–415, 1940.
21. **Seiler C, Kirkeeide RL, Gould KL.** Measurement from arteriograms of regional myocardial bed size distal to any point in the coronary vascular tree for assessing anatomic area at risk. *J Am Coll Cardiol* 21: 783–797, 1993.
22. **Skjaerpe T, Hatle L.** Noninvasive estimation of systolic pressure in the right ventricle in patients with tricuspid regurgitation. *Eur Heart J* 7: 704–710, 1986.
23. **Spaan JA.** Mechanical determinants of myocardial perfusion. *Basic Res Cardiol* 90: 89–102, 1995.
24. **Spaan JA, Breuls NP, Laird JD.** Diastolic-systolic coronary flow differences are caused by intramyocardial pump action in the anesthetized dog. *Circ Res* 49: 584–593, 1981.
25. **Sun YH, Anderson TJ, Parker KH, Tyberg JV.** Effects of left ventricular contractility and coronary vascular resistance on coronary dynamics. *Am J Physiol Heart Circ Physiol* 286: H1590–H1595, 2004.
26. **Torii R, Wood NB, Hughes AD, Thom SA, guado-Sierra J, Davies JE, Francis DP, Parker KH, Xu XY.** A computational study on the influence of catheter-delivered intravascular probes on blood flow in a coronary artery model. *J Biomech* 40: 2501–2509, 2007.
27. **Verberne HJ, Meuwissen M, Chamuleau SA, Verhoeff BJ, van Eck-Smit BL, Spaan JA, Piek JJ, Siebes M.** Effect of simultaneous intracoronary guide wires on the predictive accuracy of functional parameters of coronary lesion severity. *Am J Physiol Heart Circ Physiol* 292: H2349–H2355, 2007.
28. **Westerhof Physiological hypotheses–intramyocardial pressure N.** A new concept, suggestions for measurement. *Basic Res Cardiol* 85: 105–119, 1990.